Application of Smooth Mixed Meshes Based on Metric Identity in Aerospace Analysis and Design

Jochen Wild

DLR, Institute for Aerodynamics and Flow Technology, Lilienthalplatz 7,
D-38108 Braunschweig, Germany

Abstract. An applicable method for generating mixed meshes around simple and medium complex configurations is presented. Core part of the mesh generation strategy is a smooth meshing of the boundary layer region by structured hexahedrons and prisms applying smoothing based on solving face-weighted Laplacian equations. A preconditioning of the point set for triangulation by shear and edge-weighted average affine invariant transformation is proposed to stabilize end accelerate constrained Delaunay volume triangulation. An examples of the mesh generation strategy is shown for a generic transport aircraft in high-lift configuration.

1 Introduction

Numerical design optimization is an emerging design tool for real world applications in aerodynamics. The state of the art of 3D Navier Stokes solvers already show a good predictive capability even for more complex 3D aircraft configurations as shown for example in [1][2][3].

Optimization based on high-level computational fluid dynamics (CFD) tools using Reynolds-averaged Navier-Stokes equations (RANS) in the meantime is widely used for 2D airfoil design. Today the step towards 3D wing optimization is to be done. Although already practical for simple configurations like wing-body, the effort of calculating more complex configurations is still too high for application within an optimization environment. The main limiting factor hereby is the number of grid points necessary for accurate flow simulation using hybrid unstructured grids consisting of tetrahedral and prismatic elements. E.g. for the configuration used in the Drag Prediction Workshop [1] the medium hybrid unstructured grid used giving promising results contained approximately 12 million grid points. This resulted in a computational effort of 100 hours CPU-time on a NEC SX5 high performance computer for a given flow condition. Even the grid generation for this case took about 1 day turn-around time. This computational effort is clearly unacceptable in terms of an optimization process, where multiple configurations have to be evaluated. As a rough estimate, when assuming 200 evaluations for a converged optimization, this will lead linearly to 200 days grid generation and 800 CPU-days flow calculation. Even assuming a parallel processing of the flow on 4 processors will result in more than 1 year turn-around time for the optimization.

Regarding applications in high-lift optimization the situation worsens. Today a hybrid unstructured mesh for a transport aircraft configuration contains about 20 Million

grid points. A mesh is usually generated over night using an advancing front method for high quality meshes. Even with the new computer technology providing massively parallel LINUX cluster systems, 1 to 5 days are needed for a fully converged flow simulation. Using such meshes would require 40 to 1000 days of computing, depending on the optimization algorithm.

The big shortcoming of hybrid unstructured grids is the low anisotropy of surface triangles resulting in a large number of grid points, which is agglomerated through the number of prismatic layers for the boundary layer resolution. This low anisotropy leads to an unnecessary high resolution in spanwise direction, especially for high aspect ratio wings. Recovering the experience with the application of structured grids, it is known, that the aspect ratios of the surface quadrilaterals can be much higher, additionally resulting in well aligned body conforming meshes. The shortcoming of an overall use of structured meshes is the increasing complexity of the targeted configurations, where structured meshing reaches its limitations, mainly due to grid topology issues.

In the past the author *et al.* [4] reported a new strategy to generate mixed meshes containing smooth structured hexahedral and prismatic elements for the resolution of boundary layers by a parabolic marching routine based on the face-weighted Laplace equation. In the following the method is briefly described. New extensions are presented concerning the interface to the field triangulation and a preconditioning method for the Delaunay field triangulation. These extensions have been crucial in order to accelerate and stabilize the process. Finally the method is applied to a high-lift wing-body configuration including the use within an optimization environment.

2 Mixed Mesh Generation Methods

As long as the variations of the field variables to be resolved by the numerical solution to a set of differential equations are of the same order of magnitude in all directions the use of hybrid unstructured meshes is appropriate and furthermore avoids the manual labor of subdividing the field into blocks usually needed for structured meshes. On the other hand an adequate resolution of very thin layers with large normal gradients requires a layered structure of the mesh. Such meshes may be generated by marching away from a fixed mesh face, say the body surface in case of a boundary layer, or away from a floating mesh face in case of a wake. When the mesh on the initial face is unstructured, the resulting three-dimensional mesh extruded from it consists of prisms of triangular cross-sections and is called hybrid. A structured mesh on the initial face, of course, leads to a fully structured three-dimensional mesh.

Structured meshes are easily clustered differently in all grid line directions. Since they need far less points for directional clustering than hybrid unstructured meshes, they add efficiency to the numerical solution procedure of the differential equations. On the other hand their generation suffers from the amount of work to be invested to achieve the blocking for complex geometries. To ease the situation we combine both kinds of surface meshes starting the three-dimensional marching generation of mixed meshes simultaneously from neighboring patches with structured and unstructured surface meshes.

For the generation of these mixed meshes we integrated surface and volume triangulation methods into the DLR structured mesh generator MegaCads [5]. We used available methods, in fact the TRIANGLE code of Shewchuk [6] and the DELAUNDO code of Müller et al. [7] for surface mesh generation in parametric space. For Volume triangulation we chose the NETGEN code of Schöberl [8].

2.1 Structured Hexahedral Boundary Layer Meshes

Like in most structured mesh generation methods the 3D structured mesh blocks are initially generated by an algebraic interpolation method. Depending on the block boundaries we use either tri-linear or transfinite interpolation [9]. Since our objective is to generate smooth meshes we additionally apply smoothing with the use of elliptic equations. In the work of Niederdrenk [10] beginning with the metric identity in its differential conservative form the well known Poisson equations for structured meshes were derived including a precise analytical definition of all 9 control functions. The metric identity in its differential form simply states that the sum over the face normal vectors in the grid conforming $+\xi$ and $-\xi$ direction together with the sum over the remaining face normal vectors in η- and ζ-directions must vanish. A decomposition using the face normal vectors leads to a system of differential equations that can be separated into the face weighted Laplace equation in computational space and the so-called control functions

$$\begin{aligned}
&\underline{S}_1^2\left\{\underline{r}_{\xi\xi}+\frac{V}{\underline{S}_1^2}\left[\left(\frac{\underline{S}_1^2}{V}\right)_\xi+\left(\frac{\underline{S}_1\underline{S}_2}{V}\right)_\eta+\left(\frac{\underline{S}_1\underline{S}_3}{V}\right)_\zeta\right]\underline{r}_\xi\right\}+\\
&\underline{S}_2^2\left\{\underline{r}_{\eta\eta}+\frac{V}{\underline{S}_2^2}\left[\left(\frac{\underline{S}_2\underline{S}_1}{V}\right)_\xi+\left(\frac{\underline{S}_2^2}{V}\right)_\eta+\left(\frac{\underline{S}_2\underline{S}_3}{V}\right)_\zeta\right]\underline{r}_\eta\right\}+\\
&\underline{S}_3^2\left\{\underline{r}_{\zeta\zeta}+\frac{V}{\underline{S}_3^2}\left[\left(\frac{\underline{S}_3\underline{S}_1}{V}\right)_\xi+\left(\frac{\underline{S}_3\underline{S}_2}{V}\right)_\mu+\left(\frac{\underline{S}_3^2}{V}\right)_\zeta\right]\underline{r}_\zeta\right\}+\\
&\qquad 2\underline{S}_1\underline{S}_2\underline{r}_{\xi\eta}+2\underline{S}_2\underline{S}_3\underline{r}_{\eta\zeta}+2\underline{S}_3\underline{S}_1\underline{r}_{\zeta\xi}=0.
\end{aligned} \tag{1}$$

with the $\underline{S}_i$ being the face normal vectors

$$\underline{S}_1=\underline{r}_\eta\times\underline{r}_\zeta\,,\quad \underline{S}_2=\underline{r}_\zeta\times\underline{r}_\xi\,,\quad \underline{S}_1=\underline{r}_\xi\times\underline{r}_\eta \tag{2}$$

Prescribing the control functions, the metric identity becomes a mesh generating equation. This is used either for elliptic smoothing or for an advancing layer method through these differential equations parabolized with respect to the marching direction and subsequently discretized [11]. By this the generation of the initial algebraic mesh is not necessary.

2.2 Smooth Prismatic Boundary Layer Meshes

For unstructured meshes there exists no globally underlying computational space. Therefore, starting from the same basic principle we begin with the metric identity in its discrete form to directly derive from it the set of algebraic equations to be solved

numerically. The derivation of the equations has been shown in a previous paper of the author *et al.* [4]. Proceeding as in the structured case we decomposed the face normal vectors into the line vector directions and rewrote the metric identity in terms of line vectors with coefficients consisting of scalar products of face vectors. Compared with the expanded differential form of the identity for structured meshes, which split into the Laplacian terms and the control functions, the corresponding decomposition of the discrete form of the identity yields nothing similar, still leaving the problem to isolate the Laplacian smoothing part from the pure identity. The problem area is, of course, confined to the unstructured mesh in the body conforming surfaces. Decomposing the discrete identity for planar surfaces results in the definition of suited averages, such that the discrete Laplace equation is represented. To verify this we compared them to the discretized form of the Laplace equation for structured quadrangles and hexagonal cells [12]. So our averaging procedure is not proven but only believed to hold for any collection of triangles forming an *N*-cornered cell.

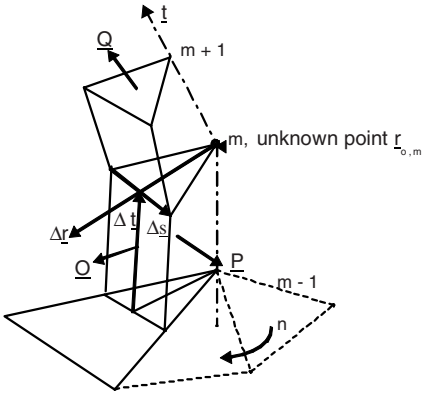

Fig. 1. Discrete triangular prism

Finally we solve equation (3) for the unknown central point $\underline{r}_0$ on level m:

$$\underline{r}_{o,m}\sum\left(\underline{\bar{O}}_n\underline{\bar{O}}_n+\frac{1}{2}\underline{\bar{Q}}\underline{\bar{Q}}_m\right)=$$
$$\sum\Big[\underline{\bar{O}}_{n,m}\underline{\bar{O}}_{n,m}\underline{rm}_{n,m}+\underline{\bar{O}}_{n,m}\underline{\bar{P}}_{n,m}\Delta\underline{s}_{n,m}+\frac{1}{4}\underline{\bar{Q}}_m\underline{\bar{Q}}_m\left(\underline{t}_{m-1/2}+\underline{t}_{m+1/2}\right) \tag{3}$$
$$+\frac{1}{4}\underline{\bar{O}}_{n,m}\underline{\bar{Q}}_{n,m}\left(\Delta\underline{r}_{m+1/2}-\Delta\underline{r}_{m-1/2}\right)+\frac{1}{4}\underline{\bar{Q}}_{n,m}\underline{\bar{P}}_{n,m}\left(\Delta\underline{s}_{m+1/2}-\Delta\underline{s}_{m-1/2}\right)\Big],$$

where $\Delta\underline{r}_{n,m}$ is defined as the midpoint between two adjacent corner points

$$\Delta\underline{r}_{n,m}=\underline{rm}_{n,m}-\underline{r}_{0,m}\quad\textbf{with}\quad\underline{rm}_{n,m}=1/2\left(\underline{rc}_{n,m}+\underline{rc}_{n+1,m}\right). \tag{4}$$

and the face and edge vectors according to **Fig. 1**.

2.3 Intermediate Layer to Connect to Volume Triangulation

In order to be able to triangulate the volume the outer hull of the hexahedrons of the structured mesh must be converted to a triangulation. First attempts to generate pyramidal elements on top of the hexahedrons led to intersections in concave regions that were only removed by using very flat pyramidal cells.

The way chosen now is a division of the outermost hexahedrons into pyramids and tetrahedrons using the center point. By this method the interface surface grid formed by the outer layer is as smooth as the hexahedral layer itself. **Fig. 2** shows the

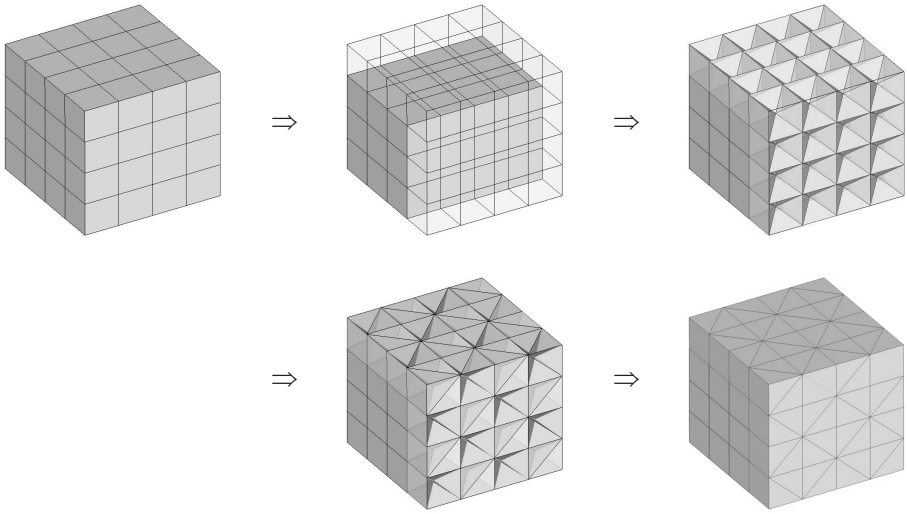

Fig. 2. Division of outermost structured hexahedrons into pyramids and tetrahedrons to achieve a smooth interface surface for tetrahedral mesh generation

sequence of dividing the outer layer first into pyramids, afterwards into tetrahedrons to form a smooth outer hull for the volume triangulation.

2.4 Preconditioned Delaunay Meshing of Tetrahedrons

For the meshing of the outer field with tetrahedrons we use the NETGEN code [8], which is a constrained Delaunay method with an advancing front for boundary recovery. One major difficulty of using structured hexahedral cells in unstructured meshes is the interface to the outer tetrahedral cells, especially if Delaunay triangulation is applied. The Delaunay criterion drives the mesh towards isotropic tetrahedrons, and by this the height of the triangle interfacing to the hexahedrons is much larger than the height of the hexahedrons. This normally results in a jump of volume size and is therefore unfavorable for the flow simulation. Another difficulty arises due to the fact that although the interface grids at the outer hexahedral layer looks smooth and well aligned, it does not fulfill the Delaunay criterion. This usually degrades the performance of the triangulation algorithm.

In order to be able to generate a suited tetrahedral mesh we use a geometric preconditioning of the surface mesh for the Delaunay algorithm. We call it preconditioning since it is a global transformation of the initial boundary triangulation in order to make it more suitable for Delaunay meshing. The volume triangulation is applied on the modified point set without major changes.

A first transformation is a shear transformation, which is important for the application to swept high aspect ratio wings of transport aircraft.

$$\boldsymbol{P}_1 = \boldsymbol{S}^{-1}\boldsymbol{P} \tag{5}$$

where $\boldsymbol{P}$ is the set of boundary points and $\boldsymbol{S}$ is the shear transformation for the wing sweep. Assuming the spanwise coordinate to be y the shear transformation is given by

$$\boldsymbol{S} = \begin{bmatrix} 1 & \sin\varphi & 0 \\ 0 & 1 & 0 \\ 0 & 0 & 1 \end{bmatrix} \tag{6}$$

where φ is the wing sweep angle. This transformation shears the surface elements and results in an intermediate mesh that is more Delaunay than the original one.

The second item to deal with is the high aspect ratio of the surface triangles. At this time anisotropic Delaunay meshing is not available. We therefore apply an edge-weighted mean affine invariant transformation. For each surface triangle an affine invariant transformation

$$\tilde{\boldsymbol{p}}_i = \boldsymbol{A}^{-1}\boldsymbol{p}_i \tag{7}$$

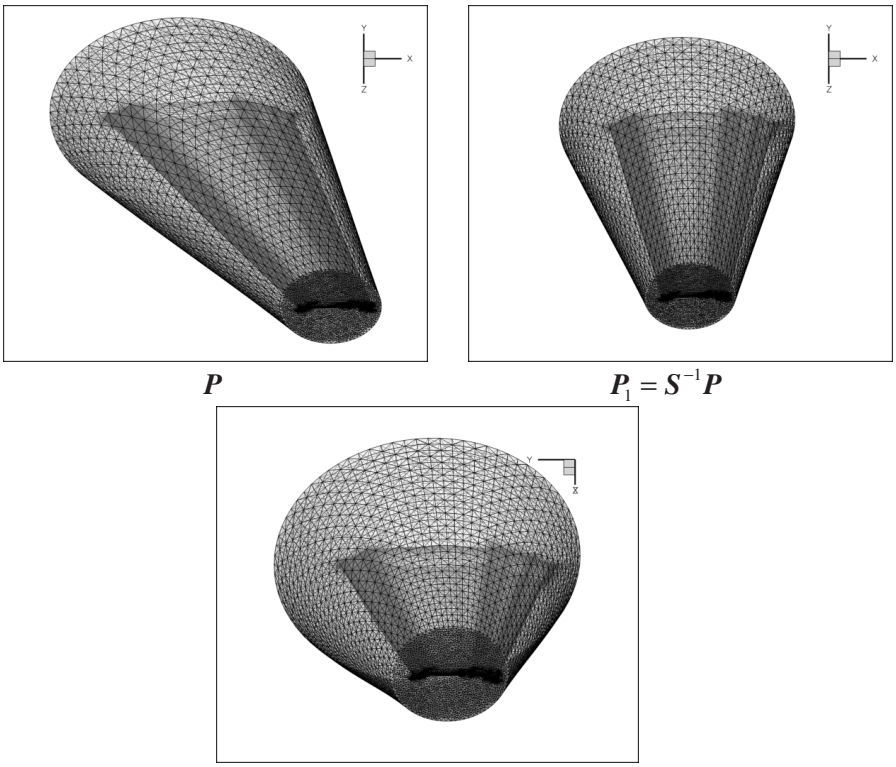

Fig. 3. Meshing box around outboard high-lift wing: top left) original geometry; top right) shear transformation applied; bottom) shear and edge-weighted affine invariant transformation applied

is defined by a matrix A reflecting the anisotropy of the surface element

$$A_{ij} = \frac{1}{n}\sum_{k=1}^{n}\left(x_{k,i} - x_{c,i}\right)\left(x_{k,j} - x_{c,j}\right) \tag{8}$$

where n is the number of points of the surface element and $\boldsymbol{x_c}$ is the center point. In fact the affine invariant is the quadratic form of an ellipsoid passing through the points of the surface element. By this the matrix reflects the size and stretching of the element. We now calculate a mean edge-weighted average of these matrices of all surface elements.

$$\overline{\boldsymbol{A}} = \sum_{i=1}^{m}\frac{n}{\sum_{j=1}^{n}\left(x_j - x_c\right)^2}\boldsymbol{A}_i \tag{9}$$

The advantage of the edge weighting is that the large regular triangles at the outer domain boundary don't mask the high anisotropy of the small surface elements at the interface. The final point array used for the Delaunay triangulation is now

$$\overline{\boldsymbol{P}} = \overline{\boldsymbol{A}}^{-1}\boldsymbol{S}^{-1}\boldsymbol{P} \tag{10}$$

In **Fig. 3** the meshing box around the outboard portion of a transport aircraft high-lift wing is shown for all steps of the preconditioning. The points-of-view are identical excluding a necessary swapping of the axes due to the affine invariant transformation where the sorting of the axes is according to the eigenvalues.

3 Application for a Generic Transport Aircraft in High-Lift Configuration

For demonstration of the mixed mesh approach using the described parabolic marching algorithms the meshing of a generic transport aircraft wing-body configuration with deployed high-lift devices is shown. This type of configuration is often too complicated for structured meshing. Especially the geometric details at the device ends and their cut-out of the main wing are very hard to be meshed with the block structured approach. On the other hand purely hybrid unstructured meshes lead to point numbers of 20 million grid points or more. For design applications these grids are therefore not suitable.

With the mesh generation strategy described in this work we are able to generate a mesh for a generic transport aircraft in high-lift configuration that contains only about 2 Mio. grid points. The wakes of all three wing elements are resolved by aligned hexahedral elements up to one half flap chord behind the flap trailing edge. Due to the parametric grid generation process, the mesh generation is applicable to geometric changes within an optimization context. The grid generation process takes about 50 minutes from scratch. Compared to the time needed to generate a classic hybrid unstructured mesh of at least 6-8 hours, there remains a significant acceleration. This time frame is acceptable for the application within an optimization framework.

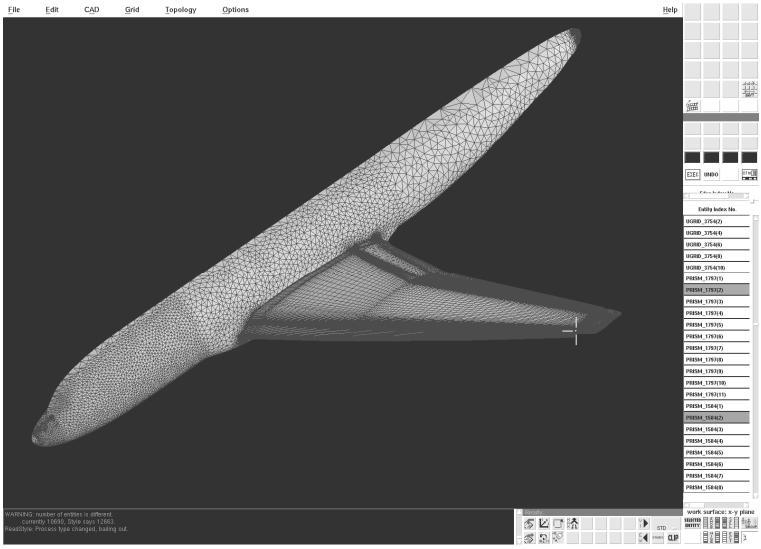

Fig. 4. View on boundary layer grid of generic transport aircraft in high-lift configuration, wing meshed with structured hexahedrons, wing tip and fuselage meshed with prisms

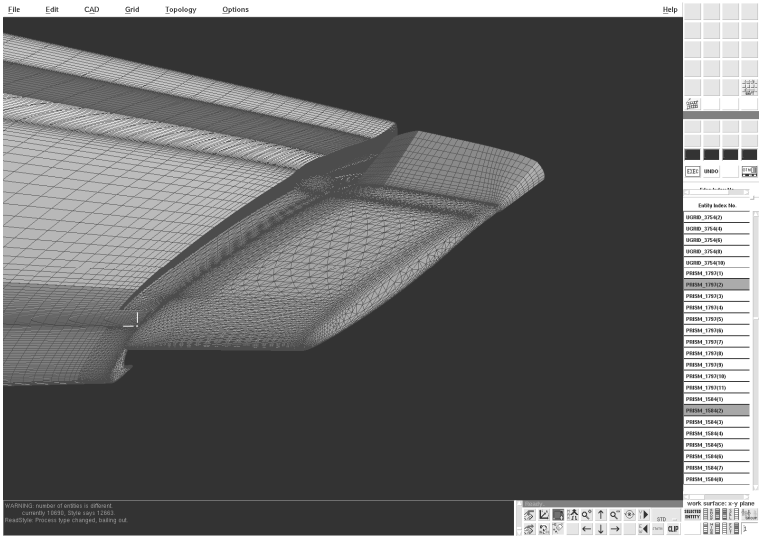

Fig. 5. Zoom on wing boundary layer grid of the generic transport aircraft in high-lift configuration with structured cells are covering boundary layers and wakes of all three wing elements and the wing tip resolved by smooth prismatic mesh.

Fig. 4 shows an overview of the boundary layer grid. Nearly the complete wing is meshed with structured type meshes. Prismatic elements are applied around the fuselage, on the wing tip and at the device ends. Additionally the wakes of all 3 wing

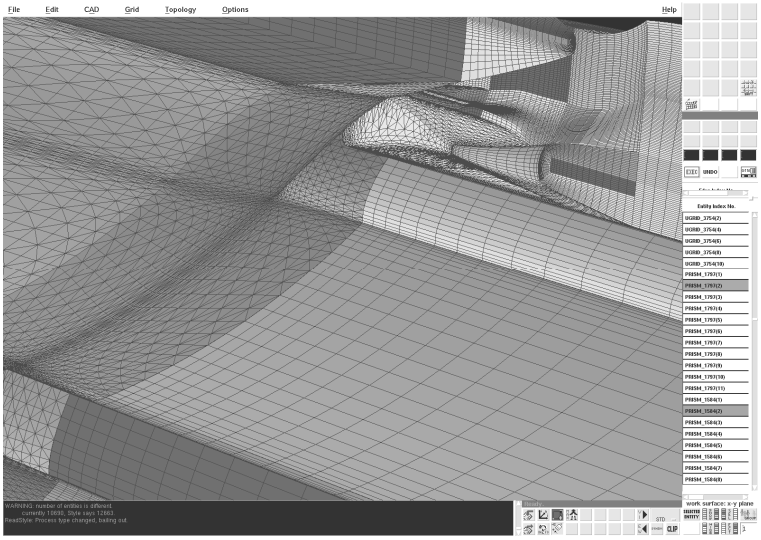

Fig. 6. Zoom on junction of main wing and outboard flap end of the generic transport aircraft showing smooth transition from hexahedral to prismatic elements and the structured wake grids

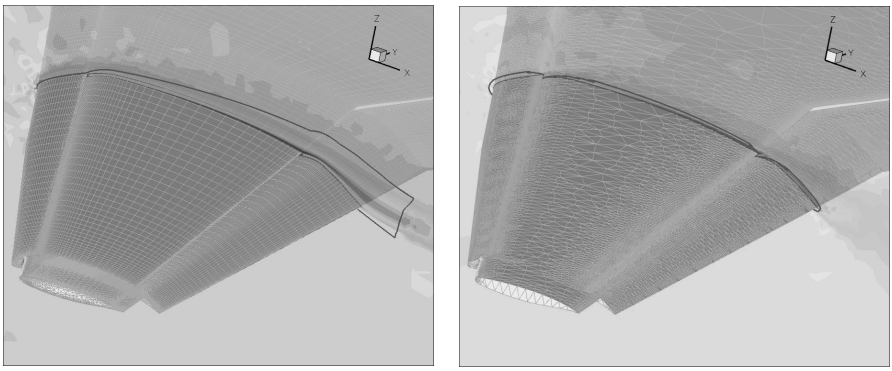

Fig. 7. Comparison of flow field around high-lift configuration at AoA 10°: left) mixed mesh; right) hybrid mesh. Contours are shown for Mach number in field and pressure coefficient on surface mesh. Solid line indicates boundary of area resolved with structured elements.

elements are captured by structured wake grids (**Fig. 5**). This is very relevant for high-lift flows, since the mixing of the shear layers has a big influence on the aerodynamic performance. **Fig. 6** shows a zoom on the device ends of the slat and the flap together with the wing cut-out in this area. A smooth transition from the structured hexahedral to the prismatic elements is observed.

For this case a comparison to a hybrid unstructured mesh containing approximately the same number of points on the surface is done. Due to the missing resolution of the wakes the overall point number of 1.5 Mio. is lower than for the mixed mesh. **Fig. 7**

shows a comparison of a cut through the flow field. The contours in the field are the local Mach number while the coloring of the surface mesh is made by the pressure coefficient. Especially the wakes of the wing elements are much better resolved with the mixed mesh.

For this configuration an aerodynamic optimization the of the positioning of slats and flaps has been performed applying the presented meshing algorithms. Within this optimization meshes were generated for 151 different configurations, while only in 13 cases the grid generation process failed. The overall optimization including mesh generation and flow simulation on a 96 CPU parallel PC cluster took about 15 days turn-around time.

4 Conclusion

An applicable method for generating mixed meshes around simple and medium complex configurations has been shown. Core part of the mesh generation strategy is a smooth meshing of the boundary layer region by structured hexahedrons and prisms applying smoothing based on solving face-weighted Laplacian equations. Special emphasis was put on the interface layer and the generation of tetrahedral elements in the outer field. A preconditioning of the point set for triangulation by shear and edge-weighted average affine invariant transformation has been proposed to stabilize end accelerate constrained Delaunay volume triangulation.

An example of the mesh generation strategy is shown for a generic transport aircraft in high-lift configuration. A superior grid accuracy compared to standard hybrid unstructured hybrid meshes with an order of magnitude less points was shown. The improved resolution of wake areas due to structured elements has been demonstrated. Finally the mesh generation strategy was successfully applied within an optimization environment.

Acknowledgements

The author dedicates this paper to Peter Niederdrenk, who has developed and implemented the theory of the face weighted Laplacian equations based on metric identity. He also is the father of the parabolic marching procedures the author uses throughout the mesh generation strategy. The author wishes Peter Niederdrenk all the best for his retirement.

References

[1] Levy, D., Zickuhr, T., Vassberg, J., Agrawal, S., Wahls, R., Pirzadeh, S., Hemsch, M.: Data summary from the first AIAA computational fluid dynamics drag prediction workshop. Journal of Aircraft 40(5), 875–882 (2003)

[2] Brodersen, O., Rakowitz, M., Amant, S., Larrieu, P., Destarac, D., Sutcliffe, M.: Airbus, ONERA and DLR results from the 2nd AIAA drag prediction workshop. AIAA Paper 2004-0391 (2004)

[3] Rudnik, R., Heinrich, R., Eisfeld, B., Schwarz, T.: DLR contributions to code validation activities within the European high lift project EUROLIFT. In: Breitsamer, C., et al. (eds.) New Results in Numerical and Experimental Fluid Mechanics IV. Notes on Numerical Fluid Mechanics, vol. 87, pp. 42–49. Springer, Heidelberg (2004)
[4] Wild, J., Niederdrenk, P., Gerhold, T.: Marching Generation of Smooth Structured and Hybrid Meshes Based on Metric Identity. In: Hanks, B.W. (ed.) Proceedings of the 14th Int. Meshing Roundtable, San Diego, CA, pp. 109–128. Springer, Berlin (2005)
[5] Brodersen, O., Hepperle, M., Ronzheimer, A., Rossow, C.-C., Schöning, B.: The Parametric Grid Generation System MegaCads. In: Proc. 5th Intern. Conf. On Numerical Grid Generation in Comp. Field Simulation, National Science Foundation (NSF), pp. 353–362 (1996)
[6] Shewchuk, J.R.: Triangle: Engineering a 2D Quality Mesh Generator and Delaunay Triangulator. In: First Workshop on Applied Computational Geometry. ACM, New York (1996)
[7] Müller, J.D., Roe, P.L., Deconinck, H.: A frontal approach for internal node generation in Delaunay triangulations. International Journal for Numerical Methods in Fluids 17(3), 241–255 (1993)
[8] Schöberl, J.: NETGEN - An advancing front 2D/3D mesh generator based on abstract rules. Computing and Visualization in Science 1, 41–52 (1997)
[9] Eriksson, L.E.: Generation of boundary-conforming grids around wing-body configurations using transfinite interpolation. AIAA Journal 20(10), 1313–1320 (1982)
[10] Niederdrenk, P.: On the Control of Elliptic Grid Generation. In: Cross, M., et al. (eds.) Proc. 6th Intern. Conf. On Numerical Grid Generation in Comp. Field Simulations, London, July 1998, p. 257. NSF Eng. Center, Mississippi (1998)
[11] Niederdrenk, P., Brodersen, O.: Controlled Parabolic Marching Grid Generation. In: Soni, B., et al. (eds.) Proc. 7th Intern. Conf. On Numerical Grid Generation in Comp. Field Simulations, Whistler, British Columbia, Canada, September 2000, p. 29. NSF Eng. Center, Mississippi, (2000)
[12] Winslow, A.: Numerical Solution of the Quasi-Linear Poisson Equations in a Non-Uniform Triangle Mesh. J. Comp. Phys. 2, 149 (1967)